

Recoil Analysis for Heavy Ion Beams

Fatih EKİNCİ¹, Erkan BOSTANCI², Özlem DAĞLI³ and Mehmet Serdar GÜZEL²

fatih.ekinci2@gazi.edu.tr, ebostanci@ankara.edu.tr, ozlemdagli@gazi.edu.tr, mguzel@ankara.edu.tr

1 Physics Department, Gazi University

2 Computer Engineering Department, Ankara University,

3 Gamma Knife Unit, Gazi University

Abstract

Given that there are 94 clinics and more than 200,000 patients treated worldwide, proton and carbon are the most used heavily charged particles in heavy ion therapy. However, there is a recent increasing trend in using new ion beams. Each heavy ion has a different effect on the target. As each heavy ion moves through the tissue, they lose enormous energy in collisions, so their range is not long. Ionization accounts for the majority of this loss in energy. During this interaction of the heavily charged particles with the target, the particles do not only ionize, but also lose energy with the recoil. Recoil occurs by atom-to-atom collisions. With these collisions, crystalline atoms react with different combinations and form cascades in accordance with their energies. Thus, secondary particles create ionization and recoil. In this study, recoil values of boron, carbon, nitrogen and oxygen beams in the water phantom were computed in the energy range of 2.0-2.5 GeV using Monte Carlo simulation and the results were compared with carbon. It was observed that there is a regular increase in the recoil peak amplitude for carbon and boron ions, unlike oxygen and nitrogen where such a regularity could not be seen. Moreover, the gaps in the crystal structure increased as the energy increases.

Keywords: Heavy ion radiotherapy, Recoil, TRIM Monte Carlo, Atom displacements

1. Introduction

Hadron beams have been used in radiation oncology for a long time due to their superior physical and biological properties compared to conventional high-energy photon beams [1, 2]. Therefore, the number of particle treatment facilities has increased significantly in the last few years, despite their cost and technological difficulties faced [3]. Protons are currently used in more than 60 facilities around the world, there are 16 centers in clinical treatments in Europe and many are under construction [4]. Based on the excellent clinical results achieved with carbon ion beams in Japan, four carbon ion therapy centers have been established in Europe in the last decade [4]. More recently, researchers have also focused on newer types of particles other than protons and carbon ions, namely helium and oxygen [5-9]. The clinical outcome of particle therapy depends on dosimetric accuracy, including accurate dose calculations and beam delivery, respectively, as well as various clinical aspects. Much of the clinical experience in particle beam therapy to date has been achieved through radiotherapy treatment planning and dose calculations based on semi-analytical pencil beam algorithms [10].

With regard to dosimetric accuracy, general purpose Monte Carlo (MC) simulations are considered the "gold standard" [11]. MC method is a statistical simulation technique developed for solving mathematical problems where finding an analytical solution is difficult. Simulation systems developed on this technique follow the traces of each particle traveling through matter one by one, based on the assumption that the quantities describing particle interactions have certain probability distributions. For many particles, quantities such as flux, energy loss and absorbed Linear Energy Transfer (LET) are recorded and average values are computed for these distributions [12]. TRansport of Ions in Matter (TRIM) simulation software developed using MC technique allows computation of all ion interactions within the target. Input parameters such as the ion type, energy, number of ions and related probabilities as well as target phantom properties including shape and material can be provided to the software. The software records all types of computed fields and can display them as needed. TRIM can compute all kinetic events and 3D distribution of ions related to energy loss processes of ions such as target damage, scattering, ionization, phonon generation and recoil. All target atom cascades in the target can be tracked in detail. The software also allows step by step analysis of all tracks [13].

The authors have identified a gap in the calculation of the recoil profiles of the heavy ions used in heavy ion therapy and the comparison of their values in the current literature. The recoil values were compared in order to find out which ions can be more effective in the treatment of tumors that are close to critical tissues. The main purpose of this study is to reveal recoil processes when all interaction processes are considered since these processes can significantly affect the efficiency in the whole heavy ion process except ionization. For this reason, the recoil values of heavy ions already used and planned to be used were evaluated using the TRIM simulation software.

The rest of the study is structured as follows: Section 2 describes the methods used in the study, followed by Section 3 where findings are presented. Section 4 presents a detailed discussion on the findings and the paper is concluded in Section 5.

2. Methods

TRIM can be used to compute detailed results of collision tables and collision cascades of each ion with atoms of the target. First, the current ion energy and depth is given and then the energy loss of the ion with the target electrons, *i.e.* the electronic stopping power called "SP", is given by the unit eV/Angstrom. Each cascade causes displacement collisions, gap generation, secondary collisions, and intermediate atom production. The number of displacement collisions indicates how many target atoms are in motion at energy above the energy of displacement. Another feature in the table is Target Gaps dedicated to the gap left behind when the rebound atom leaves its original location. A moving atom strikes a fixed target atom and transfers more than its displacement energy. If it does not have enough energy to move the first atom forward after the collision and it is the same element as the atom it hits, then no vacuum is formed [13,14].

Gaps occur in the crystal structure when the bullet atoms collide with the target atoms. The damping place of a moving rebound atom may be somewhat far from the gap it leaves [13]. When hadrons interact with the target material, only ionization does not occur. Just as bullet atoms interact with material electrons, atomic-sized collisions can also occur. Target atoms are displaced by this interaction and gaps occur in the target. In order to understand such interactions, it is necessary to explain Displacement Energy and Molecular Bonding Energy [12, 14].

Displacement energy is the energy required by a rebound atom to overcome the target's molecule binding force and remove multiple atomic gaps from their original positions. A bullet assumes that the atom has atomic number Z_1 and energy E and has the probability of a collision with an atom with atomic number Z_2 in the target. Let the energy of the bullet ion be E_1 and the energy of the atom hit E_2 after the collision. E_d , energy of displacement; E_b becomes the binding energy of a molecular atom and E_f becomes the final energy of a moving atom small enough to be considered to be at rest [13, 15].

There are 3 possibilities in the recoil reaction:

1. First, a displacement occurs at $E_2 > E_d$ (enough energy is supplied to the target atom to detach from its position). If $E_1 > E_d$ and $E_2 > E_d$ (both atoms have enough energy to leave their position) a vacuum is formed. Both atoms become mobile atoms. The E_2 energy of the Z_2 atom is reduced by E_b before another collision. If $E_2 < E_d$ then the atom being hit does not have enough energy. Atom returns to its original position by emitting E_2 energy as a photon [13].
2. Second, if $E_1 < E_d$ and $E_2 > E_d$ and $Z_1 = Z_2$, then the incoming atom is captured. E_1 oscillates as a phonon, and this collision is called a displacement collision. This type of impact is common on single element targets with large recoil cascades. If $E_1 < E_d$ and $E_2 > E_d$ and $Z_1 \neq Z_2$, Z_1 becomes an interstitial atom that forms or occupies gaps [13].
3. Finally, if $E_1 < E_d$ and $E_2 < E_d$, Z_1 becomes a transition atom and $E_1 + E_2$ energy is released as a photon. If there are several different elements in a target and each has a different energy of displacement, then E_d will change for each atom of the cascade hitting different target atoms [13].

As with photon radiotherapy, the most important problem for hadron therapy is whether the desired dose can be administered to the patient. For this, an attempt is made to determine and calibrate the correct dose using the water phantom before the patient is treated [13]. Water is the most important medium used in medical physics due to its similarity to human tissues in terms of atomic weight and density. Reliability of

stopping power calculations for water and accurate calculation of dose distribution mean accurate treatment doses for patients since the main component of the human body is considered water. In hadron therapy applications, similar to photon radiotherapy, dose distribution is controlled by tissue equivalent phantoms (such as water phantoms).

In this respect, the shape and design of the phantom structure to be used are important parameters for a simulation environment. There are various types of phantoms used for different body planning in literature [16]. In this study, a cylindrical water phantom is used (see Figure 1). In the TRIM simulation software, the atomic density of the water is 10,0222 atoms/cm³ and its density is 1g/cm³. The atomic combination ratios of hydrogen (H) and oxygen (O) atoms forming the water molecule are given as 66.6% and 33.3%, respectively. Similarly, the mass association ratios are given as 11.1% for H and 88.8% for O. The TRIM simulation program determined these percentages according to the ICRU-276 report [17].

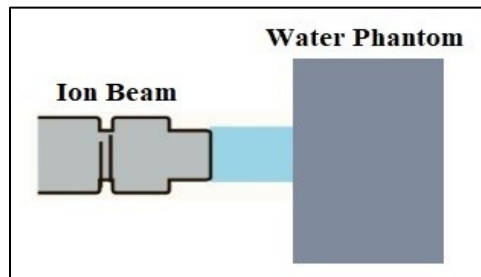


Figure 1. Water phantom

In this study, recoil values of carbon, boron, nitrogen and oxygen beams were obtained by increasing the energy in steps of 0.1 GeV in the energy range of 2.0-2.5 GeV. Results were compared using the Bragg curve of the back beam of the carbon beam and the recoil. In the calculations, the beams of carbon and boron were sent to the target in such a way that statistical deviations were in acceptable ranges.

3. Findings

In order to test the accuracy of the calculations in this study, the Bragg curves of carbons with 1.6, 2.4 and 3.0 GeV energies in the water phantom were compared with the studies in the literature [18-22]. Based on the results obtained, it was observed that the difference was approximately 4.5% (within acceptable limits i.e. $\leq 5\%$ in the medical field). The inhomogeneity effects and MC-based probabilities may sometimes result in such discrepancies, though they were within acceptable limits.

While heavy ions lose 99.8% of their energy through ionization in the target, they lose 0.02% with recoils. Recoil energies are depicted for the C, B, N and O ions for 2 GeV in Figures 2 and 3. Recoil interaction is the most important factor that changes the direction of the bullet particle, causing deviations in the direction of the advance through the target. These deviations are of great concern in tumor treatment near critical tissues.

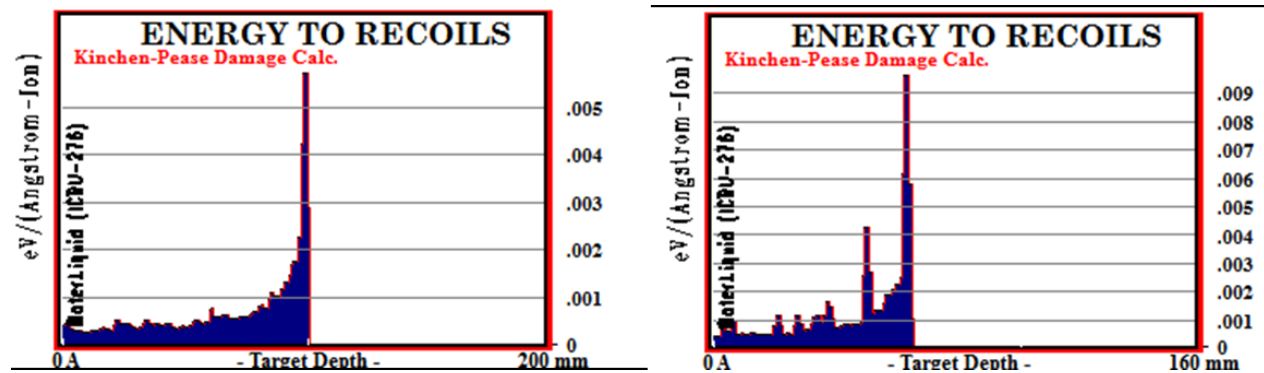


Figure 2. Ionization and recoil energies of 2.0 GeV C (left) and B (right) beams

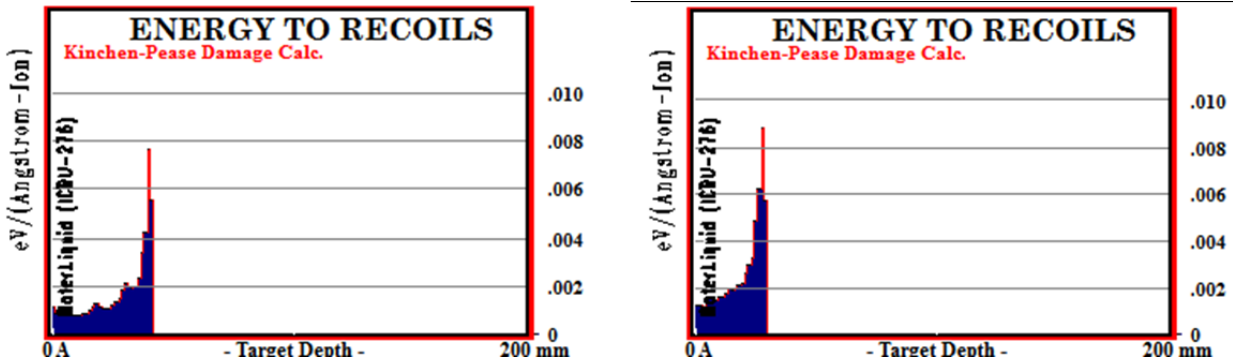


Figure 3. Ionization and recoil energies of 2.0 GeV N (left) and O (right) beams

The recoil peaks and ranges in the water phantom for the selected energy range of heavy ions are given in Table 1 and Figure 4-6. It can be seen that the range of heavy ions increases as energy increases. Maximum recoil energy is produced at the end of the range. Boron ion with the lowest mass number has the highest range. As the energy increased, the ranges for B, C, N and O ions increased 0,92 cm, 0,6 cm, 0,36 cm and 0,24 cm, respectively. Near end of range, average recoil energies produced are as follows: B ion: 3.50×10^3 eV / A-ion, C ion: 5.80×10^3 eV / A-ion, N ion: 5.35×10^3 eV / A-ion and O ion: 7.76×10^3 eV / A-ion.

Table 1. Recoil peak values (eV/A-ion $\times 10^3$), ranges (cm) and percentage differences compared with carbon produced by the beams at the target

Energy GeV	¹¹ B		¹² C		¹⁴ N		¹⁶ O	
	Recoil Peak	Range	Recoil Peak	Range	Recoil Peak	Range	Recoil Peak	Range
2	3.20	10.0	5.92	6.4	6.62	4.2	6.48	3.0
2.1	4.01	10.8	5.65	7.0	5.88	4.6	8.41	3.2
2.2	2.62	11.6	5.12	7.5	5.25	5.0	9.78	3.4
2.3	3.92	12.6	6.05	8.2	5.21	5.4	6.39	3.8
2.4	3.87	13.6	6.36	8.8	3.58	5.6	8.67	4.0
2.5	3.39	14.6	5.72	9.4	5.59	6.0	6.86	4.2

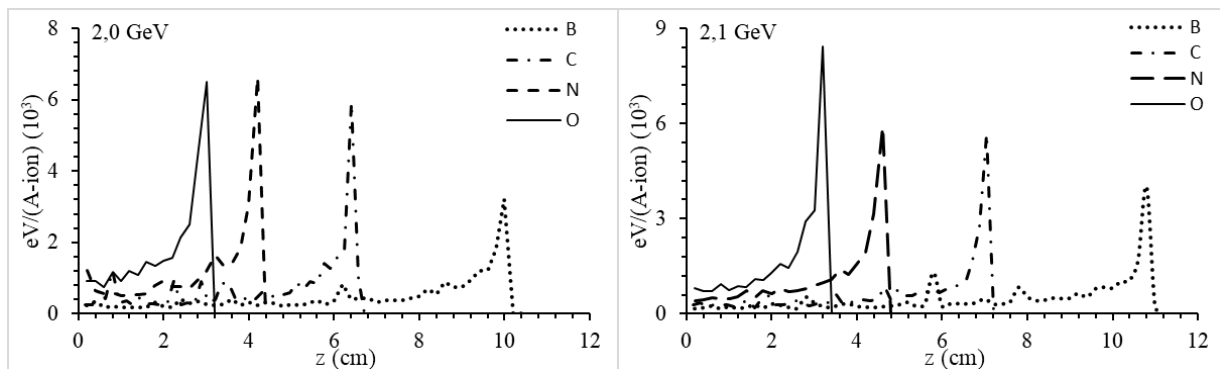


Figure 4. Change in the energy absorbed by recoil against depth in the water phantom from 2.0 and 2.1 GeV B, C, N and O beams

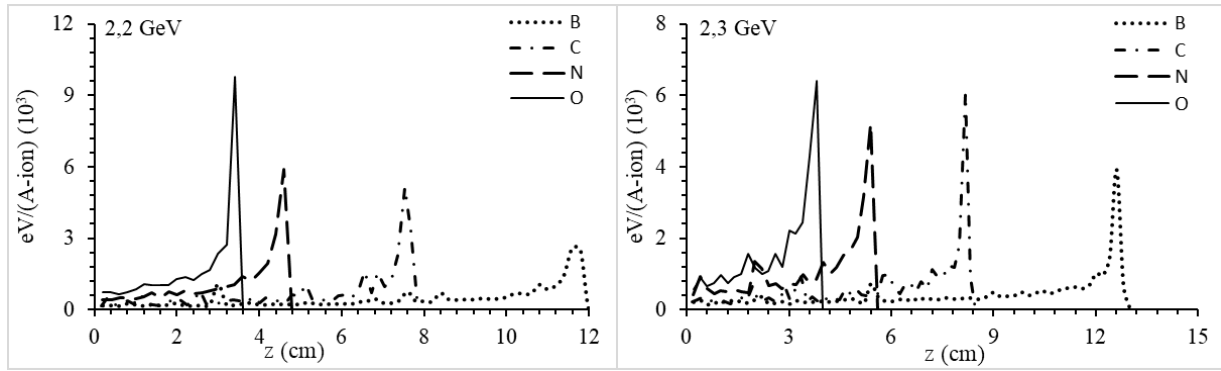


Figure 5. Change in the energy absorbed by recoil against depth in the water phantom from 2.2 and 2.3 GeV B, C, N and O beams

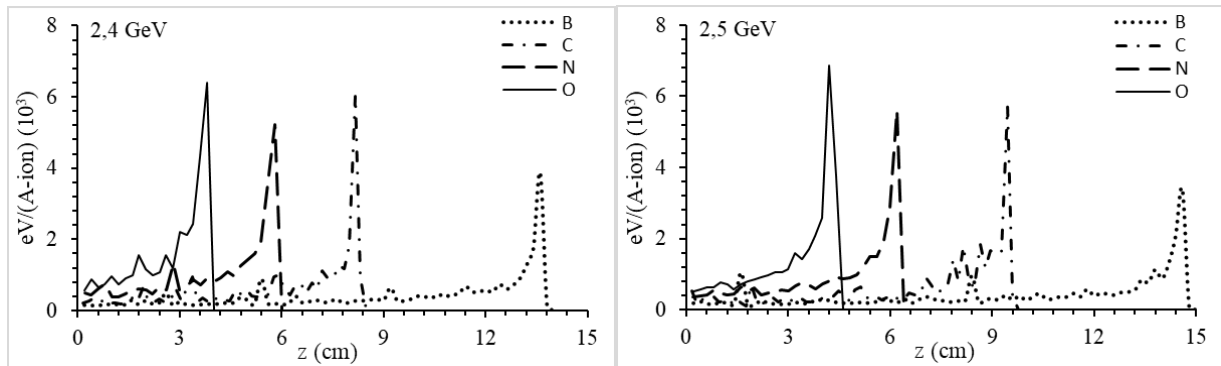


Figure 6. Change in the energy absorbed by recoil against depth in the water phantom from 2.4 and 2.5 GeV B, C, N and O beams

The gaps formed by the selected heavy ions in the crystal structure of the water are compared with those of carbon are shown in Table 2. It was observed that as the atomic number of heavy ions increases at the same energy level, the gaps they form in the crystal structure of water increase. We also observed that as the energy of the same heavy ion increases, the gaps in the crystal structure of the water increase. Since, in a water molecule, H has a displacement energy of 10 eV, a binding energy of 3 eV and surface energy of 2 eV and O has a displacement energy of 28 eV, binding energy of 3 eV and surface energy of 2 eV; the majority of the gaps formed are from H atoms. Thus, the H ion (proton) creates ionization and recoils through secondary interactions. In the energy range of 2.0 to 2.5 GeV, B, C, N and O beams created 6392, 6691, 7078 and 7668 gaps on average, respectively.

Table 2. Percentage differences of the gaps produced by the ion beams with the gaps produced by carbon

Energy (GeV)	Heavy ions				% Difference		
	¹² C	¹¹ B	¹⁴ N	¹⁶ O	¹² C- ¹¹ B	¹² C- ¹⁴ N	¹² C- ¹⁶ O
2.0	6204	5916	6573	7148	4.86	-5.62	-13.21
2.1	6402	6110	6778	7360	4.77	-5.55	-13.01
2.2	6599	6301	6980	7568	4.73	-5.46	-12.80
2.3	6793	6490	7180	7775	4.67	-5.38	-12.62
2.4	6983	6677	7375	7979	4.58	-5.31	-12.47
2.5	7169	6858	7569	8180	4.52	-5.27	-12.35
Mean	6691	6392	7076	7668	4.69	-4.43	-12.75

4. Discussion

According to the current literature in biophysics and cancer biology, it is strongly believed that heavy ion therapy should be used to guide the evolution of the therapy in the right direction [23]. There is irrefutable evidence that heavy ion therapy has significant physical, biological and dosimetric advantages over photons and proton beams. Moreover, current clinical evidence indicates promising results in many types of cancer. For this reason, there is a day-by-day increase in the construction of new therapy facilities in both number and geographical location. This increase can also be seen with the research on use of different heavy ions. Studies have focused on linear energy transfer (LET) and relative biological effect (RBE) [24-26]. In these studies, different ion combinations of the C atom have been the focus of attention [27]. The effect of heavy ions were investigated over the neutrons created by the secondary interactions, rather than LET and RBE in [28]. Research should cover the primary and secondary interactions that cause increase in dose [29] and DNA damage [30]. However, research on recoil in this area is generally limited and we have evaluated that it is not at a sufficient level in the field of medical physics [31, 32]. In this study, all interactions of heavy ions were analyzed in order to reveal the recoil interactions in the water phantom.

5. Conclusion

As there is an increase in research in heavy ion therapy, an analysis on various effects of using different heavy ions was found as a gap in the literature. This study aimed to fill this gap by providing detailed recoil interactions occurring in the target.

In this study, we compared C beams with B, N and O beams in 2.0-2.5 GeV range. Our findings have shown that C beams have 35.3% more recoil range than B beams, while it has 14.5% and 118.7% less recoil range than N and O beams, respectively. Recoil peak amplitude of C beams is 68.1% more than B beams, while it is 13.1% less than N and 22.9% less than O beams. As the energy increases, there is a gradual increase in recoil peak amplitude in C and B ions, while this pattern is irregular for N and O beams.

Considering the gaps in the crystal structure created by the beams, B beams created 4.69% less gaps than C beams. On the other hand, N and O beams have created 4.43% and 12.75% more gaps than that of C beams. We also observed a general increase in the gaps as the atomic weight and energy increase.

The authors believe that these results will guide the future research in medical physics considering various types of phantoms and biomaterials.

References

- [1] Jakel O., Karger C.P. and Debus J (2008). The future of heavy ion radiotherapy. *Medical Physics* 35, 5653-5663 ISSN 0942405.
- [2] Durante M. and Loeffler J.S. (2010). Charged particles in radiation oncology. *Nature Reviews Clinical Oncology* 7, 37-43 ISSN 1759-4774.
- [3] Newhauser W.D. and Zhang R. (2015). The physics of proton therapy. *Phys. Med. Biol.* 60 R155-209
- [4] PTCOG (2018). Particle therapy co-operative group. <https://www.ptcog.ch> accessed:20.09.2019.
- [5] Tessonnier T., Böhlen T.T., Ceruti F., Ferrari A., Sala P., Brons S., Haberer T., Debus J., Parodi K. and Mairani A. (2017). Dosimetric verification in water of a Monte Carlo treatment planning tool for proton, helium, carbon and oxygen ion beams at the Heidelberg Ion Beam Therapy Center. *Physics in Medicine and Biology* 62, 6579-6594. ISSN 1361-6560.
- [6] Tessonnier T., Mairani A., Brons S., Haberer T., Debus J. and Parodi K. (2017). Experimental dosimetric comparison of ^1H , ^4He , ^{12}C and ^{16}C scanned ion beams. *Physics in Medicine and Biology* 62 3958-3982 ISSN 0031-9155.
- [7] Fuchs H., Alber M., Schreiner T. and Georg D. (2015). Implementation of spot scanning dose optimization and dose calculation for helium ions in Hyperion. *Medical Physics* 42 5157-5166 ISSN 00942405.
- [8] Mairani A., Dokic G., Tessonnier T., Kamp F., Carlson D.J., Ciocca M., Cerutti F., Sala P.R., Ferrari A., Böhlen T.T., Jakel O., Parodi K., Debus J., Abdollahi A. and Haberer T. (2016). Biologically

optimized helium ion plans: Calculation approach and its in vitro validation. *Physics in Medicine and Biology* 61 4283-4299 ISSN 13616560.

- [9] Knausl B., Fuchs H., Dieckmann K. and Georg D. (2016). Can particle beam therapy be improved using helium ions? A planning study focusing on pediatric patients. *Acta Oncologica* 55 751-759 ISSN 1651226X.
- [10] Hong L., Goitein M., Bucciolini M., Comiskey R., Gottschalk B., Rosenthal S., Serago C. and Urie M. (1970). A pencil beam algorithm for proton dose calculations. *Physics in Medicine and Biology* 217 1305-1330 ISSN 0031-9155.
- [11] Rogers D. (2006). Fifty years of Monte Carlo simulations for medical. *Physics in Medicine and Biology* 51 R287-R301 ISSN 0031-9155.
- [12] Foster, D.G., Artur. (1982). "Average Neutronic Properties of "Prompt" Fission Products", Los Alamos National Laboratory Report LA-9168-MS.
- [13] Ziegler J.F. (2006). SRIM The stopping and range of ion in matter. <https://www.srim.org> accessed:20.09.2019.
- [14] Möller W. and Eckstein W. (1985). Ion mixing and recoil implantation by means of TRIDYN. *Nuclear Instruments and Methods in Physics Research* B7/8 645-649.
- [15] Posselt M. and Biersack J.P. (1986). Influence of recoil transport on energy-loss and damage profiles. *Nuclear Instruments and Methods in Physics Research* B15 20-24.
- [16] Behrens, R., ve Hupe, O. (2016). Influence of the phantom shape (slab, cylinder or alderon) on the performance of an hp(3) eye dosimeter. *Radiation Protection Dosimetry* (2015), pp. 1–9.
- [17] ICRU (1979). International Commission on Radiation Units and Measurements. Average Energy Required to Produce an Ion Pair, ICRU Report 31 (International Commission on Radiation Units and Measurements, Bethesda, MD).
- [18] Ekinci F. (2019). Investigation of Interactions of Proton and Carbon Beams With Tissue Equivalent Targets. *Gazi University Graduate School of Natural and Applied Sciences* 102-105.
- [19] Archambeau, J. O., Bennett, G. W., Levine, G. S., Cowen, R., ve Akanuma, A. (1974). Proton radiation therapy. *Radiology*, 110, 445-457.
- [20] Carlsson, Å. K., Andreo, P., and Brahme, A. (1997). Monte Carlo and analytical calculation of proton pencil beams for computerized treatment plan optimization. *Physics in Medicine & Biology*, 42(6), 1033.
- [21] Fippel, M., ve Soukup, M. (2004). A Monte Carlo dose calculation algorithm for proton therapy. *Medical Physics*, 31(8), 2263-2273.
- [22] Medin, J., ve Andreo, P. (1997). Monte Carlo calculated stopping-power ratios, water/air, for clinical proton dosimetry (50-250 MeV). *Physics in Medicine & Biology*, 42(1), 89.
- [23] Mohamad O., Yamada S. and Durante M. (2018). Clinical indications for carbon ion radiotherapy. *Clinical Oncology* 30 317-329.
- [24] Combs S.E. (2018). Proton and Carbon Ion Therapy of Intracranial Gliomas. *Innovative Treatment Modalities. Prog Neurol Surg. Basel, Karger*, 32, 57–65.
- [25] Buizza G., Molinelli S., D'Ippolito E., Fontana G., Pella A., Valvo F., Preda L., Orecchia R., Baroni G. and Paganelli C (2019). MRI-based tumour control probability in skull-base chordomas treated with carbon-ion therapy. *Radiotherapy and Oncology* 137, P32-37.
- [26] Dahle T.J., Magro G., Ytre-Hauge K.S., Stokkevåg C.H., Choi K. and Mairani A. (2018). Sensitivity study of the microdosimetric kinetic model parameters for carbon ion radiotherapy. *Physics in Medicine & Biology* 63 225016.
- [27] Hartfiel S., Häfner M., Perez R.L., Rühle A., Trinh T., Debus J., Peter E. Huber P.E. and Nicolay N.H. (2019). Differential response of esophageal cancer cells to particle irradiation. *Radiation Oncology* 14, 119.
- [28] Han Y., Tang X., Geng C., Shu D., Gong C., Zhang X., Wu S. and Zhang X. (2019). Investigation of in vivo beam range verification in carbon ion therapy using the Doppler Shift Effect of prompt gamma: A Monte Carlo simulation study. *Radiation Physics and Chemistry* 162, 72-81.
- [29] Wang Q., Antony A., Deng Y., Chen H., Moyers M., Lin J. and Yepes P. (2019). A track repeating algorithm for intensity modulated carbon ion therapy. *Physics in Medicine and Biology*, 64, 9.
- [30] Brownstein J.M., Wisdom A.J., Castle K.D., Mowery Y.M., Guida P.M., Lee C., Tommasino F., Tessa C.L., Scifoni E., Gao J., Luo L., Campos L.D.S., Ma Y., Williams N., Jung S., Marco Durante M. and Kirsch D.G. (2018). Characterizing the potency and impact of carbon ion therapy in a

primary mouse model of soft tissue sarcoma. American Association for Cancer Research 1-30 DOI: 10.1158/1535-7163.MCT-17-0965.

- [31] Choi K.D., Mein S.B., Kopp B., Magro G., Molinelli S., Ciocca M. and Mairani A. FRoG—A New Calculation Engine for Clinical Investigations with Proton and Carbon Ion Beams at CNAO. *Cancers* 10(11), 395 DOI: <https://doi.org/10.3390/cancers10110395>.
- [32] Spooner N.J.C., Majewski P., Munac D., Snowden-Ifftd D.P. (2010). Simulations of the nuclear recoil head–tail signature in gases relevant to directional dark matter searches. *Astroparticle Physics*, 34, Issue 5, December 2010, Pages 284-292